

# Self-tensioning system for long-span wooden structural floors

J. Estévez-Cimadevila<sup>1</sup>, D. Otero-Chans<sup>1</sup>, E. Martín-Gutiérrez<sup>1</sup>, F. Suárez-Riestra<sup>1</sup>

(1) University of A Coruña, Department of Architectural, Civil and Aeronautical Building Structures, Campus A Zapateira, 15071, A Coruña, Spain.

Corresponding author: [javier@udc.es](mailto:javier@udc.es) (Javier Estévez-Cimadevila)

ORCID: <https://orcid.org/0000-0002-8460-2097> (Javier Estévez-Cimadevila)  
<https://orcid.org/0000-0003-1738-252X> (Dolores Otero-Chans)  
<https://orcid.org/0000-0001-7464-4288> (Emilio Martín-Gutiérrez)  
<https://orcid.org/0000-0002-8839-5611> (Félix Suárez-Riestra)

**ABSTRACT:** A patented self-tensioning system for long-span wooden structural floors is described that increases the performance of the deflected sections in terms of both resistance and deformation. The system is based on a force multiplier mechanism composed by two connecting rods which are secured to a post-stressing tendon. The mechanical device is activated by the transmission of the load from the structural element to the supports, causing an elongation and stressing the tendon. This transmission comes with a slight vertical displacement of the supports. Throughout this system, the intensity of the tensioning force varies with the applied load; thus, a more favorable bending moment distribution from the load is obtained, and the relative deformations of the different sections of the piece are reduced. This article presents a comparative study of the structural behavior of p-shape cross section wooden structural floors with spans from 9 m to 18 m, comparing sections with and without pre-stress, and sections with the self-tensioning system.

**KEYWORDS:** Pre-stressing; Self-tensioning; Post-tensioning; Wooden floors; Long-span.

## 1. Introduction

Pre- and post-stressing systems are widely known and utilized in structural design to limit the tension stresses from deflections. These systems were originally developed for concrete, to alleviate the virtually non-existent tension resistance of concrete through pre-compression. The first patents are attributed to Eugène Freyssinet in 1920, although some previous experiments are known that date back to the end of the XIX century. Nowadays, the use of these systems has been generalized, extending to the structural design for other materials, such as steel and wood.

It is well known that in defect-free wood, the resistance to tension is greater than the resistance to compression. However, the presence of defects in real wooden structures (knots, cracks, deviations in the fibres, etc.) significantly limits their resistance to tension. While compression failures are ductile and produced by flattening the fibres, failure from tension is associated with brittle fracture, which is undesirable in building structures. Therefore, pre- and post-stressing systems offer a two-fold advantage in the design of wooden structures. On the one hand, the redistribution of stresses reduces the tension stress, which is more limiting for resistance. On the other hand, as a consequence of the previous point, the probability of a brittle fracture of the piece is reduced.

The pre-stressing of wooden structural elements is traditionally achieved through the use of bonded tendons in the form of bars, plates, or bands. These reinforcing elements are normally constructed of either metallic elements [1-2] or fibre reinforced polymers (FRPs) [3-4]. The tendons are subjected to tension stresses prior to attachment to the wood using adhesives. After curing the adhesive joint, the initial axial stress is removed and the reinforcing elements introduce a pre-compression in the section to which the tendon is attached, emulating traditional pre-stressed concrete systems. If this pre-compression is applied eccentrically to the section, the result is a bending of the element used as a precamber, which, in addition to modifying the stress distribution, also improves the deflection behavior of the beams. The reinforcements also provide rigidity to the section, especially when steel tendons are utilized [1]. One of the primary problems of these adherent reinforcements is the occurrence of delamination at the ends of the beam caused by the concentration of stress at the edges of the adhesive joints [5].

Because of this problem, wood post-stressing systems with non-adherent tendons have also been recently studied. In these systems, the stress can be introduced after the elements have been installed. These systems have been evaluated for their application in structural elements [6-8] in terms of rigidity and their behavior in post-stressed frames during earthquakes [9-10].

In this article, a novel post-stressing system is presented. It differs from the existing systems in that the axial stress is automatically generated as a function of the load to which the structural element is subjected. In this way, it is possible to modify the stress distribution and the deformation of the element as a function of the load state of the structure. The system is initially proposed for long-span wooden structural floors, although it may be applied to any horizontal structure and for any structural material.

## 2. Description of the system

The high performance of wood-derived materials and the advances in material technology enable the design of long-span wooden structural elements. Because it is

difficult to fabricate rigid connections in wood, the elements usually are mounted on two supports, which is an inefficient solution in terms of resistance and deformation. In these cases, the decisive design criterion usually meets the deformation limitations. One of the options for partially countering this problem consists of fabricating elements with an initial precamber. This solution is efficient if the design of the section is conditioned by deformation limitations according to the construction appearance criterion. It may also be an adequate solution when the magnitude of the variable loads is small and the design of the piece is conditioned by the deformation limitations to ensure the integrity of the constructive elements.

Because of this limitation, an initial precamber is only truly efficient for light roofs. Therefore, in structural floors with significant variable loads, the use of an initial precamber does not solve the problem, and it becomes necessary to gain rigidity using more elevated heights to meet the deformation conditions.

In this article, an alternative solution is presented. This solution consists of a novel patented self-tensioning system, which significantly increases the bending efficiency of pieces mounted on two supports. The system is based on the introduction of an eccentric post-stressing force on the structural element. The tension is introduced automatically, i.e., without the need for hydraulic jacks or any auxiliary machinery for post-stressing. It is obtained by transforming the loads transmitted to the supports into a tensing force via a load-multiplying device. In this manner, the self-tensioning force varies as a function of the loads to which the structure is subjected during its service life, increasing and decreasing simultaneously with the change of the load. The eccentric tension gives rise to a negative bending moment, whose magnitude varies with those of the acting loads. This achieves a continuous redistribution of the moments and a significant reduction of the relative deformations among the different sections of the piece. This noticeable improvement of the structural behavior permits the use of reduced height in long-span structural floors.

Hydraulic or mechanic devices can be utilized for multiplying the load. Although multiple designs can be used to achieve the multiplying effect, in this article, a very simple solution is presented. This simple system consists of connecting rods (Figs. 1 and 2), in which the transmission of the load from the structural element to the supports produces an elongation and tension of the tendon which is secured to the device. The deformation suffered by the mechanic device when bearing the loads gives rise to a vertical displacement on the supports of the structural element. Therefore, the self-tensioning force and the seat of the supports depend on the geometry used for the multiplying mechanism and on the rigidities of the elements.

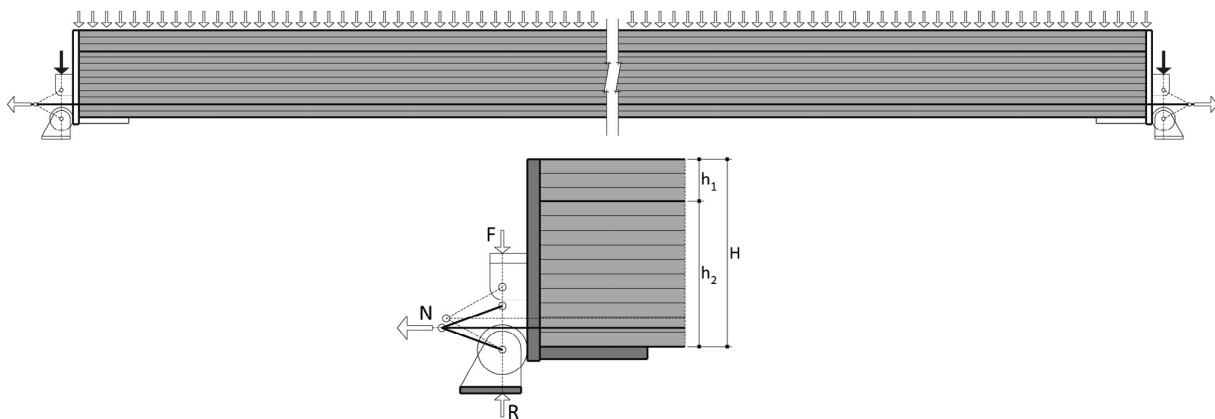


Fig. 1. Force-multiplying device based on a system of connecting rods.

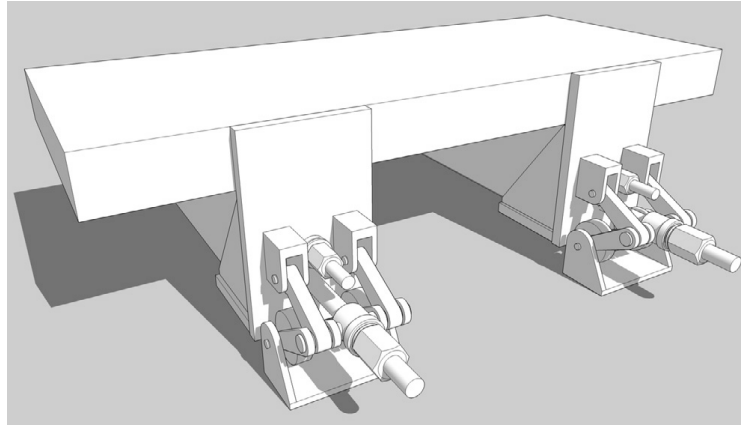


Fig. 2. Virtual image of the multiplying device based on a system of connecting rods.

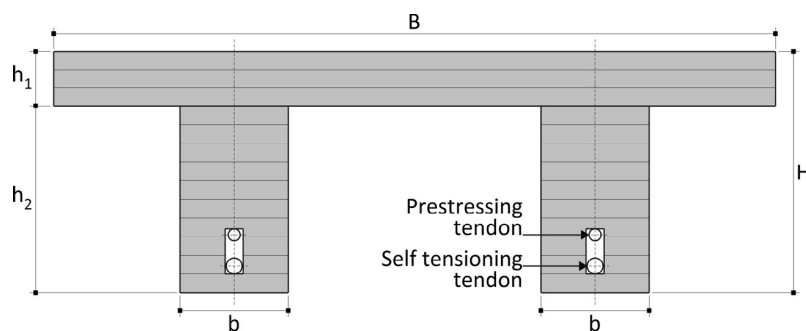


Fig. 3. Wooden piece with  $\pi$  type cross section.

### 3. Materials and analysis

To illustrate the advantages of pre-stressing and of the proposed self-tensioning system, the structural behavior of long-span wooden structural floors with the following characteristics was analyzed:

- Spans of 9, 12, 15 and 18 m.
- Cross section of  $\pi$  type, formed by two laminated wood ribs, GL28h strength class according to the classification established in EN 14080:2013 [11], and a cross laminated timber top plank [12] (Fig. 3). This type of cross section was chosen for two reasons. Firstly, a greater eccentricity is achieved for the stressing element with respect to the barycenter of the homogenized section comparing  $\pi$  section with a homogenized rectangular section. This leads to a larger negative bending moment generated by the eccentric axial force and, therefore, to an increase in system efficiency. Secondly,  $\pi$  section is easier to prefabricate in a shop, which resolves the entire horizontal structure (bearing ribs and beam layout) into a single piece.
- A permanent load  $G_k$  of 1 kN/m<sup>2</sup> is considered, corresponding to the coatings and the self-weight of the structural system ( $W_k$ ). Given that these long-span solutions are generally associated with public buildings, two scenarios are analyzed for the determination of the variable load:

Administrative and public use zones with furniture:  $Q_k = 3$  kN/m<sup>2</sup> (Factor for quasi-permanent value of a variable action  $\Psi_2 = 0.3$ )

Commercial and public use zones without obstacles:  $Q_k = 5$  kN/m<sup>2</sup> ( $\Psi_2 = 0.6$ )

- Dimensions of the section (Fig. 3): Ribs of 180-mm width ( $b$ ) and various heights ( $h_2$ ), depending on the piece span, are analysed. The ribs are equipped with a middle groove to accommodate the tensioning elements. The cross-laminated top plank has dimensions of 1200 x 90 mm<sup>2</sup> ( $B \times h_1$ ). The 1200-mm width takes optimal advantage of the standard plank dimensions. The 90-mm thickness satisfies both the structural needs of the beam layout and the minimum thickness necessary to be considered in the calculation of the section resistance. The total height length  $H$  of the section is determined in terms of the span  $L$  of the piece as follows:

$$\text{Live load } Q_k = 3 \text{ kN/m}^2 \quad H = L/33$$

$$\text{Live load } Q_k = 5 \text{ kN/m}^2 \quad H = L/30$$

These height/span ratios result in slender pieces, verifying the efficiency of the system.

- Two tensioning rods are used. They can be threaded or unthreaded, with square or circular cross sections. One of the rods is used for the initial pre-stressing, and the other is activated by the self-tensioning system. The area of the self-tensioning system rod ( $\Omega$ ) is increased by the height of the structural floor, and with the magnitude of the acting loads, such that its work stress is similar for the different case studies. As shown in Fig. 3, the tensioning rods are placed inside a groove near the lower edge of the section, leaving only the minimum necessary distance to guarantee additional fire protection. The fabrication of the groove is not complicated. It can be done in several ways: building the  $\pi$  floor ribs through two glued elements, whose width is  $b/2$  and where the groove has been previously machined; building double ribs of  $b/2$  width, whose separation allows the tendon to pass in between; machining the groove in the lower part of an element and later gluing the rib's inferior layer.
- As for behavior of pre-stressing tendons in case of fire, it should be noted that their arrangement in channels inside of the wood allows to use the wood as an insulating, protection element. Fire is not a determining aspect in the tensioned solution since the purpose of the self-tensioned system is to improve the structural behavior from the point of deformations. As proven in the analyzed cases, the non pre-stressed element has a sufficient resistant capacity to comply with the ultimate limit state requirements. Fire is an extraordinary situation where it is not necessary to comply with the deformation regulatory requirements. Therefore, the contribution of self-tensioning system to the overall resistance can be omitted.
- The self-tensioning system uses connecting rods with an initial angle  $\alpha = 30^\circ$  (Fig. 4).

Table 1 summarizes the geometric characteristics and the load values for the structural floors in this study.

For the purpose of determining the efficiency of the pre-stressing in general, and of the self-tensioning system in particular, a comparative analysis of the 8 pieces (F1-F8) described in Table 1 is performed for 4 conditions as follows:

- S1. Non-pre-stressed section, with no initial precamber.
- S2. Non-pre-stressed section, with a geometric precamber of  $L/500$ .
- S3. Pre-stressed section to a precamber of  $L/500$ .
- S4. Pre-stressed section to a precamber of  $L/500$ , and the self-tensioning system.

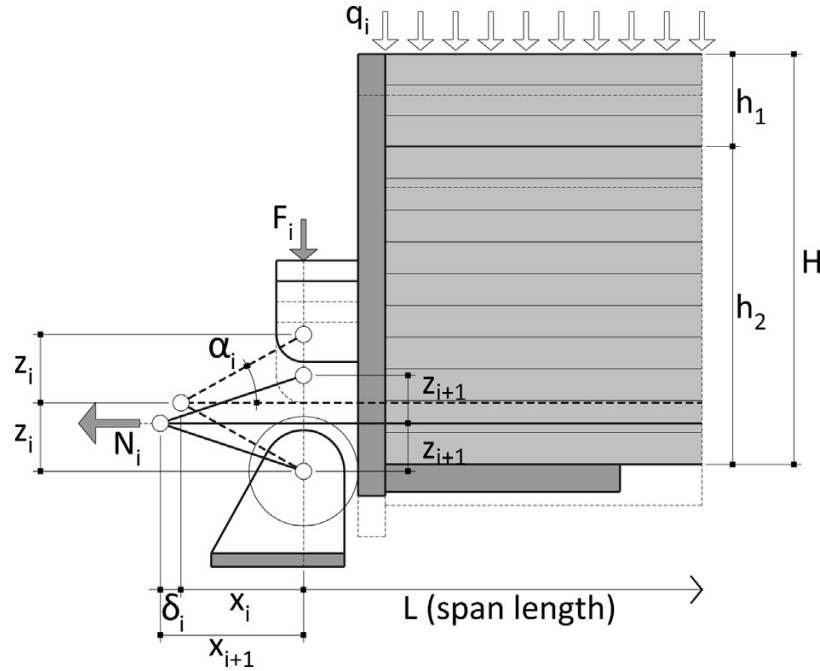


Fig. 4. Displacements of the multiplying device under a load.

Table 1: Geometric characteristics and load values of the structural floors.

Type	Geometry of the p-type structural floor						Self-tensioning tendon area X (mm <sup>2</sup> )	Considered actions			
	L (m)	H (mm)	h <sub>1</sub> (mm)	h <sub>2</sub> (mm)	B (mm)	b (mm)		Self-weight Wk (kN/m <sup>2</sup> )	Permanent load Gk (kN/m <sup>2</sup> )	Live load Qk (kN/m <sup>2</sup> )	Quasi-permanent live load w <sub>2</sub> ·Qk (kN/m <sup>2</sup> )
F1	9	270	90	180	1200	180	500	0.77	1.77	3.00	0.90
F2	12	360	90	270	1200	180	700	0.92	1.92	3.00	0.90
F3	15	450	90	360	1200	180	900	1.07	2.07	3.00	0.90
F4	18	540	90	450	1200	180	1100	1.22	2.22	3.00	0.90
F5	9	300	90	210	1200	180	700	0.84	1.84	5.00	3.00
F6	12	400	90	310	1200	180	900	1.00	2.00	5.00	3.00
F7	15	500	90	410	1200	180	1100	1.16	2.16	5.00	3.00
F8	18	600	90	510	1200	180	1300	1.32	2.32	5.00	3.00

In long-span timber floors, the dimensions are fundamentally determined by the deformation limitations and problems of vibration. From the deformation point, the most restrictive conditions are the following:

- The integrity of the construction elements, which limits the relative deformation produced after placing the element in service. This condition must be verified for the characteristic combination of actions [13]:

$$\sum_{j \geq 1} G_{kj} + P + Q_{k,1} + \sum_{i > 1} \psi_{0,i} Q_{k,i}$$

The limit varies according to the regulations of different countries, although in most cases, and in the technical literature, it is recommended not to exceed L/500 when using fragile elements, such as partitions, continuous dropped ceilings, or rigid jointless floors.

- Construction appearance, which must be verified for the quasi-permanent combination of actions [13]:

$$\sum_{j \geq 1} G_{k,j} + P + \sum_{i > 1} \Psi_{2,i} Q_{k,i}$$

The limit value usually adopted by regulations is  $L/300$ , although there are differences in the limitations established by different countries, as mentioned above.

$G_{k,j}$	Characteristic value of permanent action j
$P$	Relevant representative value of a pre-stressing action
$Q_{k,1}$	Characteristic value of the leading variable action 1
$Q_{k,i}$	Characteristic value of the accompanying variable action i
$\Psi_{0,i}$	Factor for combination value of a variable action
$\Psi_{2,i}$	Factor for quasi-permanent value of a variable action

The combined effect of creep and humidity generates an increase in the permanent deformation produced by loads on the wood. This creep deformation ( $u_{creep}$ ) is determined from the instantaneous deformation ( $u_{inst}$ ) considering a deformation factor ( $k_{def}$ ) of 0.6, according to the Eurocode 5 [14] for service class 1 corresponding to interior structures.

$$u_{creep} = k_{def} u_{inst}$$

As for the timber floor's problems of vibrations, all consulted works about are circumscribed to the usage of solid timber solutions. No relevant research has been found in relation to the effect that pre-stressing may have on this material. Nevertheless, the vast number of available references on this issue for other materials [15-17] reports a significant increment of the element's fundamental frequency due to the positive effect provided by the tensioning force. Although, the high slenderness achieved with the self-tensioning system would make decisive the vibration control when dimensioning non pre-stressed elements. The consideration of the tensioning's positive effect and the incidence of damping factors makes the compliance of regulatory requirements perfectly viable. However, the importance of this problem requires further detailed research that exceeds the objective of this article.

For the determination of the tensioning force, successive load increases produce a variation of the multiplying device geometry, generating a non-linear effect that increases with the load. This non-linear effect is positive from the perspective of post-stressing because the load increase translates into a greater multiplying effect ( $\lambda$ ) and, thus, a larger tensioning force. To include this geometric non-linearity, the calculations are performed using an incremental load process, where the multiplying effect corresponding to each deformation state is considered.

Self-tensioning force at instant  $i$ :

$$N_i = \lambda_i F_i = \frac{2}{\text{tg} \alpha_i} F_i = \frac{x_i}{z_i} q L \quad (1)$$

Elongation of the tendon at instant  $i$ :

$$\delta_i = \frac{L + 2x_i}{2E\Omega} N_i \quad \delta_i = \frac{L + x_i}{E\Omega} N_i \quad (2)$$

New multiplier:

$$\lambda_{i+1} = 2 \frac{x_i + \delta_i}{z_i - \sqrt{z_i^2 - 2x_i \delta_i - \delta_i^2}} \quad (3)$$

The elastic deformations of the connecting rods are not included in the analysis of the multiplying effect ( $\lambda$ ) of the device because they are negligible in comparison to the

elongation of the tendon. The elastic shortening generated on the wooden piece by the axial pre-stressing is also neglected. The elastic shortening of the wood is significantly reduced due to the high axial rigidity of the piece. In any case, its effect is positive on the deflection of the piece. This positive effect is because the shortening of the wooden piece is not accompanied by a relaxation of the tendon; on the contrary, the deformation of the self-tensioning device increases, and as a consequence of the non-linear effect, the tensioning force and its associated moment increase.

#### 4. Results and Discussion

Figure 5 graphically indicates the measurement criteria of the deflection ( $\omega$ ), that is the difference between the displacement of mid-span of the element ( $u$ ) and the vertical displacement (seat) of the supports ( $s$ ).

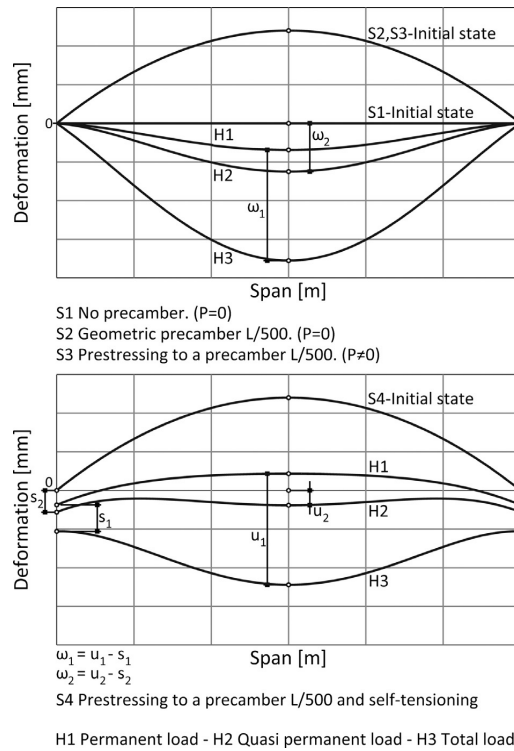


Fig. 5. Deformations  $x_1$  (integrity of the construction elements) and  $x_2$  (construction appearance) for S1–S4 sections.

Two situations are analyzed: deflection compliance with the criteria of constructive element integrity ( $\omega_1$ ), through relative deformation produced between the permanent load and the total load hypothesis; deflection compliance for the criteria of construction appearance ( $\omega_2$ ), through relative deformation of the structural element under the quasi-permanent load hypothesis. The values are obtained from the deformations corresponding to 3 combinatory load hypotheses.

H1. Permanent load: 
$$\sum_{j \geq 1} G_{k,j} + P_c + P_{self}$$

H2. Quasi-permanent load: 
$$\sum_{j \geq 1} G_{k,j} + P_c + P_{self} + \Psi_{2,i} Q_{k,1}$$

H3. Total load: 
$$\sum_{j \geq 1} G_{k,j} + P_c + P_{self} + Q_{k,1}$$

- $P_c$  Relevant representative value of pre-stressing action
- $P_{self}$  Relevant representative value of self-tensioning action



Table 2 shows a summary of the results corresponding to the deflection values ( $\omega$ ) obtained for a variable live load  $Q_k$  of  $3 \text{ kN/m}^2$ .

Table 2: Deflections ( $x$ ) for structural floors with variable live loads of  $3 \text{ kN/m}^2$ .

Deformation conditions	Structural floor type	Height (mm)	Span (m)	S1	S2	S3	S4	Deflection (mm)	Relative deflection		
				Non-pre-stressed section No precamber	Non-pre-stressed section Geometric precamber I/500	Pre-stressed section Precamber L/500	Pre-stressed section and self-tensioning Precamber L/500				
Integrity of the construction elements ( $x_1$ )	F1	270	9	38	L/237	38	L/237	28	L/321	17	L/529
	F2	360	12	52	L/231	52	L/231	38	1/316	22	L/545
	F3	450	15	67	L/224	67	L/224	49	L/306	27	L/556
	F4	540	18	82	L/220	82	L/220	61	L/295	33	L/545
Construction appearance ( $x_2$ )	F1	270	9	37	L/243	19	L/474	8	L/1125	3	L/3000
	F2	360	12	51	L/235	27	L/444	12	L/1000	2	L/6000
	F3	450	15	67	L/224	37	L/405	19	L/789	1	L/15000
	F4	540	18	84	L/214	48	L/375	26	L/692	1	L/18000

Following the criterion of constructive element integrity ( $\omega_1$ ), which is usually the most restrictive in terms of dimensions, the data in Table 2 show that the height obtained from the proposed slenderness ratio ( $H=L/33$ ) is insufficient when the non-pre-stressed wooden sections are used. This is because the relative deflections vary from  $L/237$  to  $L/220$ . Table 2 also shows that fabricating pieces with an initial precamber does not affect the result because the deformation affecting integrity constructive elements is independent of the existence of a precamber. The results improve when the precamber is achieved through pre-stressing. This improvement is from the significant reduction of the creep deformation of the piece as a result of the beneficial effect of the negative moment generated by the eccentric axial pre-stressing. This reduction varies from  $38-28=10 \text{ mm}$  for  $L=9 \text{ m}$  and from  $82-61=21 \text{ mm}$  for  $L=18 \text{ m}$ . However, even with this improvement, the relative deflections for the S3 case ( $L/321$  to  $L/295$ ) are unacceptable in terms of guaranteeing the absence of damage in the coatings. Finally, the combination of an initial pre-stressing and the self-tensioning system (S4) substantially modifies the results. The relative deflections are reduced to  $L/529$  ( $L=9 \text{ m}$ ) and  $L/545$  ( $L=18 \text{ m}$ ). These values satisfy the regulatory demands of particularly sensitive damageable elements, such as partition walls. The placement of the self-tensioning system can improve the results compared with pre-stressing alone. Consequently, for  $L=9 \text{ m}$  and  $L=18 \text{ m}$  the deflections for the pre-tensioned section are 65% and 85% bigger comparing to those obtained with the self-tensioned system.

The second deformation condition analyzed corresponds to the construction appearance ( $\omega_2$ ). For this condition, obtaining a precamber from either the fabrication of the pieces or through an initial pre-stressing process aids in achieving acceptable values. However, the efficiency of the self-tensioning system is verified when a design that practically maintains horizontality is achieved, as shown in Table 2. The displacement difference between the supports and the mid-span reaches a value of only 3 mm in the worst situation analyzed, corresponding to F1 floor typology.

The presented results and the efficiency of the system for a slenderness of  $H=L/30$  are visualized in the deformation plots in Figs. 6 to 9. These figures show the results for spans of 12 and 18 m as an example, corresponding to the 3 acting load combinations (H1 to H3) described above.

The shaded areas in the plots correspond to the zones where the deformations of the self-tensioned pieces are localized during service, defined by the quasi-permanent combination and the total load situation.

Figures 6 and 7 show the deformation results of the non-pre-stressed case (S1), and the case with pre-stressing and the self-tensioning system (S4). The difference in behavior in the service situation between these two cases is remarkable. For the 12-m pieces (Fig. 6), the non-pre-stressed solution (S1) yields a deflection of 22 mm for a permanent load and 74 mm for the total load, representing a relative drop of 52 mm between the two conditions. In contrast, in the solution featuring the self-tensioning system (S4), under the same circumstances, the displacement changes from -4 mm to 24 mm, reducing the change between the conditions to 28 mm, that is, the drop is reduced by 46% of the non-pre-stressed value. The result is even more important if we also consider the seat of the supports and analyze the deflection, which is the effect that may generate damage in the construction elements. In this case, the sample starts at a deflection of -8 mm for the permanent load and changes to 14 mm for the total load, representing a relative decrease of only 22 mm for a span of 12 m ( $L/545$ ).

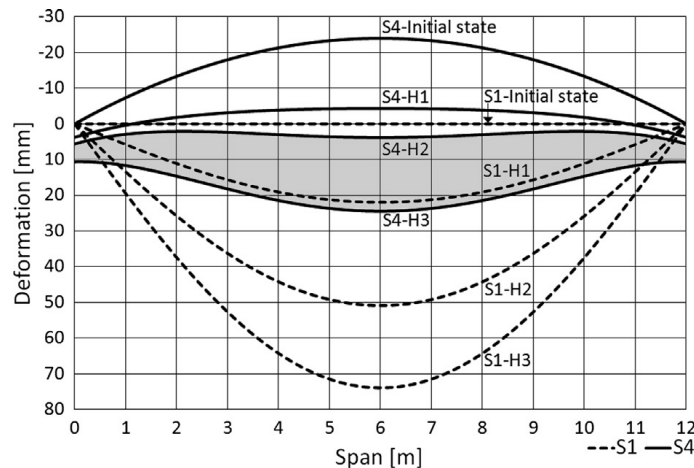


Fig. 6. Deformation comparison for S1 and S4 sections.  $L = 12$  m;  $w_2 = 0.3$ ;  $Q_k = 3$  kN/m<sup>2</sup>.

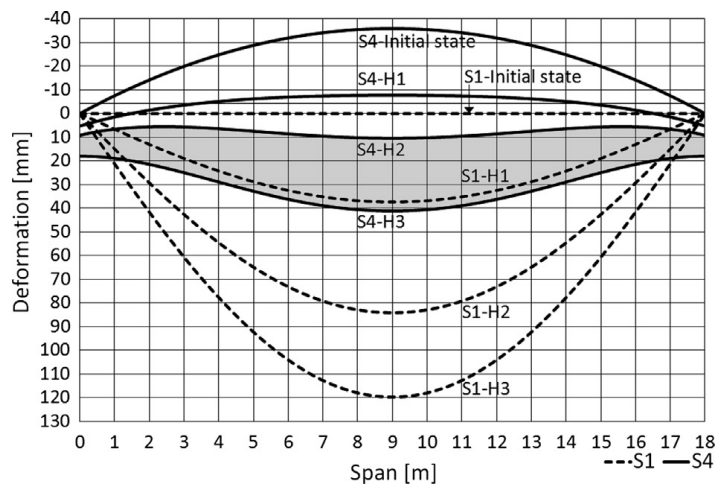


Fig. 7. Deformation comparison for S1 and S4 sections.  $L = 18$  m;  $w_2 = 0.3$ ;  $Q_k = 3$  kN/m<sup>2</sup>.

Therefore, the vertical displacement at the supports occurred when the self-tension system bears the load provokes a significant reduction in floor's deformations. These are the ones that most often provoke cracking damage in weak partitions and finishing elements. The existence of these displacements in the supports should not raise any problem under a constructive point of view. The relevant displacement is the one happening in the structure's service situation. This is the difference of displacements at the supports between the permanent load and total load hypothesis. This value has a very small magnitude (reaching a maximum of 8 mm for the case of elements spanning 18 meters). Therefore, the movement is easily assumable using any kind of joint coverage in the affected elements.

The data in Fig. 7 show similar results for the case of the 18-m span pieces. In the non-pre-stressed solution (S1), the relative displacement between the permanent load case and the total load case is 82 mm (38 mm to 120 mm). In the case of the self-tensioning system (S4), the displacement is reduced to 49 mm (-8 mm to 41 mm). In terms of distorsion, taking into account the seat of the supports, the deflection is reduced to 33 mm for a span of 18 m ( $L/545$ ). On the other hand, the difference in the support displacement between the permanent load and the total load hypothesis reaches 8 mm. This is perfectly assumable by a joint coverage element.

Figures 8 and 9 compare the pre-stressed sections (S3) and sections that are also coupled to the self-tensioning device (S4). Once again, the data show a substantial improvement in behavior with a tensioning force that varies with the acting load. During service, the appropriate post-stressing is continuously provided to minimize the relative deflections of the piece. In this case, increasing the tensioning force of the self-tensioning system allows the design of the piece to remain minimally distorted, even with the variation of the live load. In the case of the pre-stressed solution (no self-tensioning system) (S3), the relative deflection for a 12 m span (Fig. 8) is  $L/1000$  for the quasi-permanent load hypothesis (H2), and is  $L/333$  for the total acting load (H3). These values are reduced to  $L/6000$  and  $L/867$  by utilizing the self-tensioning system (S4). Analyzing the situation for a span of 18 m (Fig. 9), the comparative results are similar. The pre-stressed solution (S3) returns values of  $L/692$  (quasi-permanent load-H2) and  $L/290$  (total load-H3). In contrast, with the self-tensioning system (S4) the values are reduced to  $L/18000$  and  $L/777$ .

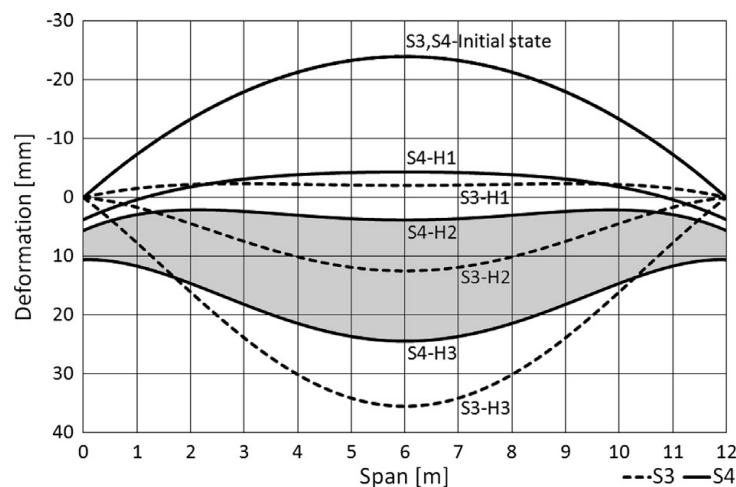


Fig. 8. Deformation comparison for S3 and S4 sections.  $L = 12$  m;  $w_2 = 0.3$ ;  $Q_k = 3$  kN/m<sup>2</sup>.

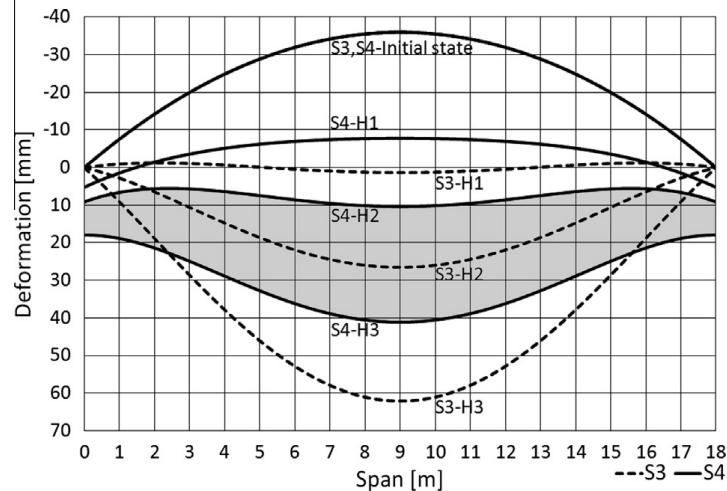


Fig. 9. Deformation comparison for S3 and S4 sections.  $L = 18$  m;  $w_2 = 0.3$ ;  $Q_k = 3$  kN/m<sup>2</sup>.

Table 3 shows deflections obtained for a variable live load  $Q_k$  of 5.00 kN/m<sup>2</sup>. In this case, because the case is commercial or public use, a higher coefficient  $\Psi_2 = 0.6$  is used for the determination of the quasi-permanent variable load fraction, as established in the regulations [13].

Table 3: Deflections ( $x$ ) for structural floors with variable live loads of 5 kN/m<sup>2</sup>.

Deformation conditions	Structural floor type	Height (mm)	Span (m)	S1 Non-pre-stressed section No precamber		S2 Non-pre-stressed section Geometric precamber L/500		S3 Pre-stressed section Precamber L/500		S4 Pre-stressed section and self-tensioning Precamber L/500	
				Deflecti on (mm)	Relative deflection	Deflecti on (mm)	Relative deflection	Deflecti on (mm)	Relative deflectio (mm)	Deflection (mm)	Relative deflectio
Integrity of the construction elements ( $x_1$ )	F5	300	9	47	L/191	47	L/191	37	L/243	17	L/409
	F6	400	12	64	L/187	64	L/187	50	1/240	22	L/429
	F7	500	15	83	L/181	83	L/181	65	L/231	27	L/441
	F8	600	18	103	L/175	103	L/175	82	L/220	33	L/450
Construction appearance ( $x_2$ )	F5	300	9	47	L/191	29	L/310	18	L/500	3	L/2250
	F6	400	12	64	L/187	40	L/300	26	L/462	2	L/2400
	F7	500	15	83	L/181	55	L/273	37	L/405	1	L/1875
	F8	600	18	103	L/175	72	L/250	51	L/353	1	L/1500

The load increase is compensated with a slight reduction of the slenderness by adopting a value of  $H=L/30$  for the height, instead of the previously used value of  $H=L/33$ . Following the criterion of construction element integrity, the obtained height is insufficient in the case of non-pre-stressed wood. The relative deflections in this case vary from  $L/191$  to  $L/175$ . The problem persists even when the pieces are fabricated with an initial precamber, because the deformation produced that affects the integrity of the constructive elements is independent of this initial precamber. By pre-stressing the piece, a significant reduction of the relative deflection is obtained, reaching  $L/243$  to  $L/220$ . This reduction is  $47-37=10$  mm for  $L=9$  m and  $103-82=21$  mm for  $L=18$  m. However, this improvement is still insufficient and leads to deformation conditions that do not guarantee the absence of damage in the

construction elements. Finally, considering the solution including the self-tensioning system, the relative deflection is reduced to values between  $L/409$  and  $L/450$ . These values are satisfactory because the consideration of a  $5 \text{ kN/m}^2$  variable load does not include the presence of partition walls. For the only pre-stressed cross section's case (S3), the vertical deflections are 68% and 105% greater comparing to those obtained with the self-tensioning system (S4) when considering  $L=9 \text{ m}$  and  $L=15 \text{ m}$  respectively.

With regard to deformations for the condition of construction appearance, the results verify the efficiency of the system. As shown in Table 3, the trace of the deformation outline remains nearly horizontal, with a displacement difference between the supports and the mid-span reaching 12 mm in the worst case analyzed, corresponding to an 18 m span.

Figures 10 and 11 show the deformations corresponding to spans of 9 and 15 m for the same 3 load states described above. The shaded areas in the figures show the range of deformation corresponding to the service condition for pieces with the self-tensioning system.

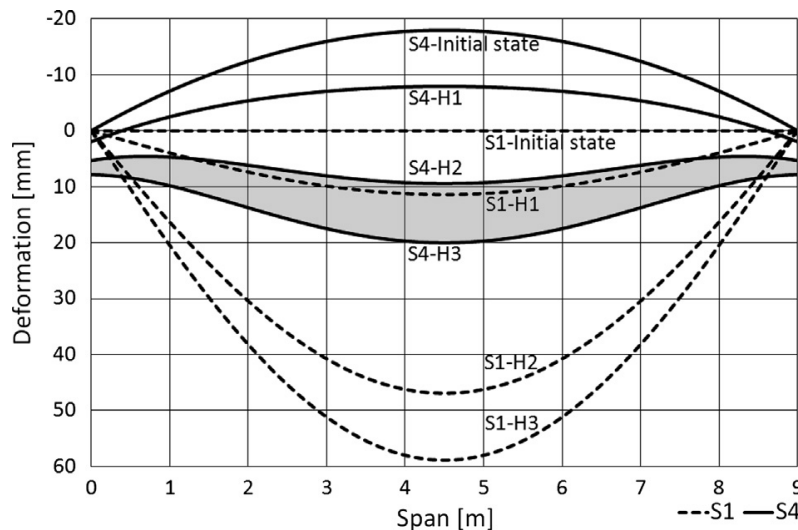


Fig. 10. Deformation comparison for S1 and S4 sections.  $L = 9 \text{ m}$ ;  $w_2 = 0.6$ ;  $Q_k = 5 \text{ kN/m}^2$ .

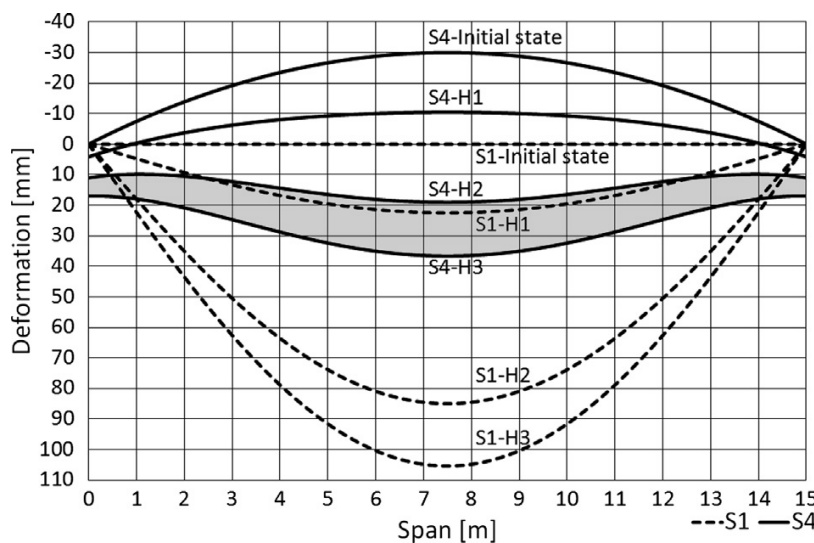


Fig. 11. Deformation comparison for S1 and S4 sections.  $L = 15 \text{ m}$ ;  $w_2 = 0.6$ ;  $Q_k = 5 \text{ kN/m}^2$ .

Figures 10 and 11 compare the deformations of non-pre-stressed pieces (S1) and pieces with the self-tensioning system (S4). The plots illustrate the efficiency of self-tensioning, which produces a remarkable reduction in deformation, and permits structural floor to remain nearly horizontal in service conditions even though it is slender. The relative deflection of the non-pre-stressed piece (S1) of the 9-m span piece (Fig. 10) is between  $L/191$  (quasi-permanent load-H2) and  $L/153$  (total load-H3). In contrast, with the self-tensioning system (S4) the corresponding values are reduced to  $L/2250$  and  $L/741$ . The situation is similar for the 15-m span piece (Fig. 11). The relative deflection for the total load of the non-pre-stressed solution reaches  $L/143$ , and is reduced to  $L/764$  in the presence of the self-tensioning system.

The results corresponding to both variable live load values considered in the analysis (3 kN/m<sup>2</sup> and 5 kN/m<sup>2</sup>) are also compared. The data show that for a load of 5 kN/m<sup>2</sup>, the improvement in terms of deformation  $\omega_1$  produced by the pre-stressed solution (S3) as compared to the non-pre-stressed wood (S1) is lower than that obtained for the 3 kN/m<sup>2</sup> load. For 3 kN/m<sup>2</sup>, the range of improvement goes from 26% to 27%, whereas for the 5 kN/m<sup>2</sup> load, the corresponding values are 20% and 22%. This is because the initial tensioning force is limited to the value corresponding to a precamber of  $L/500$ . Therefore, for a section with a given geometry, the tensioning force is the same for different values of the variable live load. The variable load increase is produced maintaining the same initial pre-stressing force; this translates into an efficiency loss, since the instantaneous deformations corresponding to a load increase are the same as those of a non-pre-stressed piece (S1).

A completely different situation exists with the self-tensioning system (S4). Because the tensioning force introduced by the multiplying mechanism increases with the load in a non-linear fashion, the consequence is an increase in efficiency. The effect of the efficiency is shown by the data in Tables 2 and 3. If we analyze the deformation values corresponding to the condition of construction element integrity, the data show that, while the relative deflection is worse for longer spans (both for non-pre-stressed and pre-stressed sections), the situation is reversed with the self-tensioning system, i.e., the relative deflection improves with the span. This is because longer spans increase the value of the force transmitted to the supports, and, as a consequence of the non-linear effect, the tensioning force becomes greater.

The improvement introduced by the self-tensioning system is also manifested in resistance, because the bending stress redistribution generated by the eccentric axial tensioning significantly increases its load capacity.

Figures 12 and 13 show the bending moments calculated for the following load hypotheses.

H1. Permanent load:

$$\sum_{j \geq 1} \gamma_{G,j} G_{k,j} + \gamma_{Pc} P_c + \gamma_{Pself} P_{self}$$

H3. Total load:

$$\sum_{j \geq 1} \gamma_{G,j} G_{k,j} + \gamma_{Pc} P_c + \gamma_{Pself} P_{self} + \gamma_{Q,i} Q_{k,i}$$

$\gamma_{G,j}$	Partial factor for permanent action j
$\gamma_{Pc}$	Partial factor for pre-stressing action
$\gamma_{Pself}$	Partial factor for self-tensioning actions
	Equal to $\gamma_{G,j}$ or $\gamma_{Q,1}$ , depending on the self-tension generating force.
$\gamma_{Q,1}$	Partial factor for variable action 1

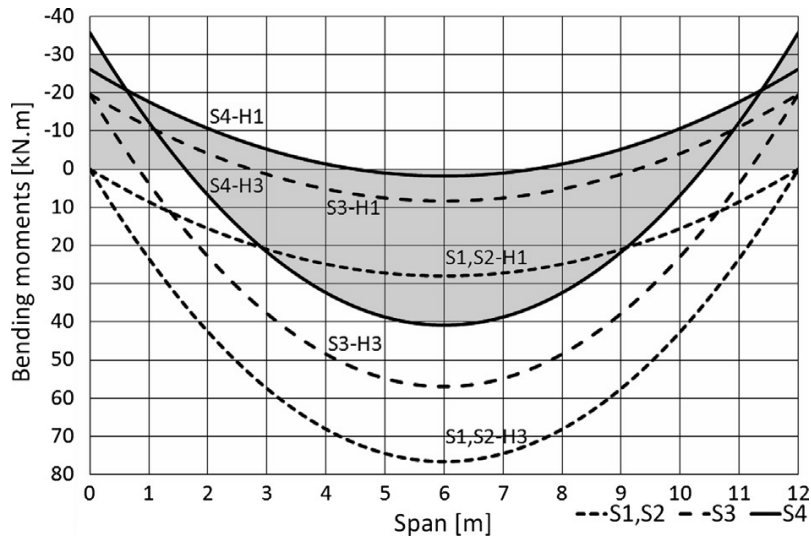


Fig. 12. Comparison of bending moments for S1, S2, S3 and S4 sections.  $L = 12$  m;  $Q_k = 3$  kN/m<sup>2</sup>.

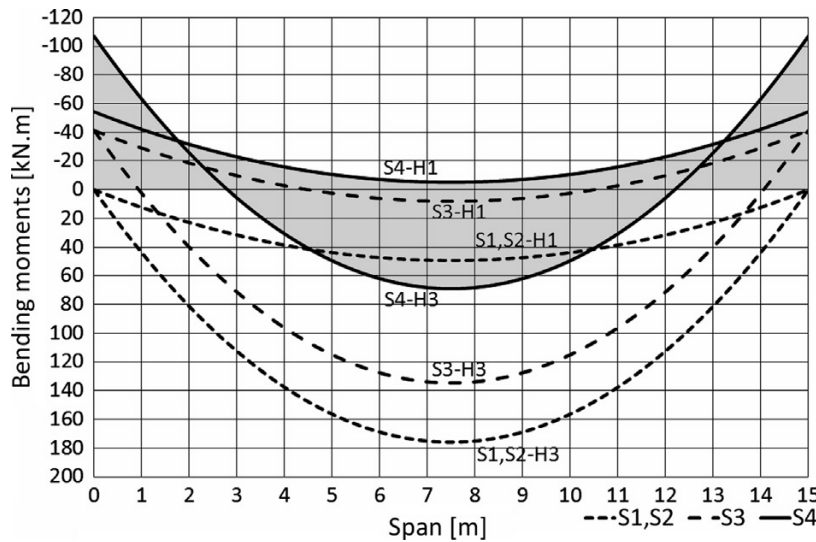


Fig. 13. Comparison of bending moments for S1, S2, S3 and S4 sections.  $L = 15$  m;  $Q_k = 5$  kN/m<sup>2</sup>.

The load values are shown in Table 1. The envelopes of the bending moments for both hypotheses are shaded in the figures for the case of the self-tensioning system to aid in visualizing the redistribution effect produced in the bending from the load.

The results verify the efficiency of the proposed system. The data in Fig. 12 show that, for a positive moment of 76.59 m·kN (isostatic value) in the non-pre-stressed solution, and with or without a precamber (S1 and S2), the self-tensioning system (S4) redistributes the bending stresses into negative moments of 35.76 m·kN, and a positive moment of 40.83 m·kN. These represent percentages of 47% and 53% with respect to the isostatic value. When the span is increased to 18 m, there is a redistribution of the bending stresses, yielding negative moments of 106.92 m·kN (59%) and a positive moment of 75.05 m·kN (41%). This increase in the percentage of negative moments produced by the redistribution is a consequence of the increase in tensioning force produced by the non-linearity. As the load increases, the multiplying effect (X) increases.

Similar results are obtained when the variable load is increased to 5 kN/m<sup>2</sup>. For a 9 m span piece, the moment distribution percentages between negative and positive are 52% negative and 48% positive, and 61% and 39% for a 15-m span piece (Fig.13). Therefore, in all the cases analyzed, the negative bending moments oscillate between 47% and 61% of the corresponding isostatic value. This verifies the stress redistribution efficiency of combining pre-stressing with self-tensioning as a function of the acting load.

The consequence of the bending moment redistribution is an increase in the load capacity of the structural element. Table 4 shows a summary of the total surface load values utilized for the estimation of actions in the structural analysis and the values of the ultimate surface load corresponding to the non-pre-stressed sections (S1) and the sections with the self-tensioning system (S4). Those ultimate surface load values correspond to the surface load values wherein the more limiting characteristic value of the material property is reached. In pieces without pre-stressing, the ultimate load corresponds in all cases to the bending resistance. In the case of pre-stressed sections, the most limiting ultimate load is obtained to the flexo-compression resistance, except for the case with a span of 18 m, whose dimensions are conditioned by shear stress.

The data in Table 4 show that using the self-tensioning system significantly increases the surface load value for which the ultimate stress is reached. In non-pre-stressed sections (S1), the ultimate load oscillates between 2.20 and 2.75 of the design load. With the self-tensioning system (S4), significantly superior values are reached, i.e., 3.70 to 5.28 of the initial design load. As a consequence, the improvement produced by the variable self-tensioning system in the cases analyzed, with respect to non-pre-stressed sections, vary from 63% to a maximum of 117%. This translates into a significant increase in safety.

Table 4: Values of the design surface load and ultimate load.

Type	Span	Total height	Total load Action estimation	Ultimate load <b>S1</b>	Ultimate load <b>S4</b>	$\frac{q_{u,S1}}{G_k+Q_k}$	$\frac{q_{u,S4}}{G_k+Q_k}$	$\frac{q_{u,S4}}{q_{u,S1}}$
				Non-pre-stressed sections	Self-tensioning sections			
	<b>L</b> (m)	<b>H</b> (mm)	<b>G<sub>k</sub>+Q<sub>k</sub></b> (kN/m <sup>2</sup> )	<b>q<sub>u, S1</sub></b> (kN/m <sup>2</sup> )	<b>q<sub>u, S4</sub></b> (kN/m <sup>2</sup> )			
F1	9	270	4.77	13.10	25.20	2.75	5.28	1.92
F2	12	360	4.92	13.10	23.60	2.66	4.80	1.80
F3	15	450	5.07	13.10	22.40	2.58	4.42	1.71
F4	18	540	5.22	13.10	21.40	2.51	4.10	1.63
F5	9	300	6.84	16.10	35.00	2.35	5.12	2.17
F6	12	400	7.00	16.10	31.30	2.30	4.47	1.94
F7	15	500	7.16	16.10	28.90	2.25	4.04	1.79
F8	18	600	7.32	16.10	27.10	2.20	3.70	1.68

## 5. Conclusions

A self-tensioning system based on the placement of a force-multiplying mechanism connected to the tensioning tendons is proposed, which activates automatically with the load placed on the structural element. One of its greatest advantages is that the intensity of the tensioning force varies with the magnitude of the applied loads. The



application of the system to wooden pieces with  $\pi$  type cross sections permits a much more favorable distribution of the load bending moments. In this way, a high efficiency is achieved in resistance, especially in deformations. Therefore, the system is especially suitable for long-span structural floors.

Structural floors of  $\pi$  type were analyzed, with 9 to 18 m spans and heights of L/33 and L/30, for variable live loads of 3 kN/m<sup>2</sup> and 5 kN/m<sup>2</sup>.

The self-tensioning system achieves an efficient redistribution of bending moments. In the cases analyzed, the negative bending moments ranged from 47% to 61% of the corresponding moment of the isostatic beam.

The self-tensioning system demonstrated an increase in the load capacity with respect to non-pre-stressed sections, from 63% to a maximum 117%.

From the perspective of system deformations, the self-tensioning system permits a virtually negligible deflection during service. In the acting hypothesis of the permanent load and the quasi-permanent fraction of the variable load, corresponding to the usual condition of the structure, the relative deflection values varied within the range from L/1500 to L/18000.

## Acknowledgments

This study forms part of a research project entitled “High-performance prefabricated systems of pretensioned wood laminate with non-bonded tendons”, financed by the Ministry of Economy and Competitiveness of the Kingdom of Spain and the European Fund for Regional Development.

## References

- [1] A. Borri, M. Corradi, Strengthening of timber beams with high strength steel cords, *Compos. B* 42 (2011) 1480–1491. <https://doi.org/10.1016/j.compositesb.2011.04.051>
- [2] V. De Luca, C. Marano, Prestressed glulam timbers reinforced with steel bars, *Constr. Build. Mater.* 30 (2012) 206–217. <https://doi.org/10.1016/j.conbuildmat.2011.11.016>
- [3] Z.W. Guan, P.D. Rodd, D.J. Pope, Study of glulam beams pre-stressed with pultruded GRP, *Comput. Struct.* 83 (2005) 2476–2487. <https://doi.org/10.1016/j.compstruc.2005.03.021>
- [4] A. Yusof, A.L. Saleh, Flexural strengthening of timber beams using glass fibre reinforced polymer, *Electron. J. Struct. Eng.* 10 (2010) 45–56.
- [5] A. Brunner, M. Schnüriger, Strengthening timber beams with prestressed artificial fibres: the delamination problem, in: *COST C12 Final Conference Proceedings*, 1, A.A. Balkema Publishers, 2005, ISBN 0415366097, pp. 219–224.
- [6] A. Buchanan, A. Palermo, D. Carradine, S. Pampanin, Post-tensioned timber frame buildings, *Struct. Eng.* 89 (17) (2011) 24–30.
- [7] W. Van Beerschoten, A. Palermo, D. Carradine, S. Pampanin, Design procedure for long-span post-tensioned timber frames under gravity loading, in: *Proceedings of the 12th World Conference on Timber Engineering (WCTE)*, 1, Pierre Quenneville, 2012, ISBN 978-1-62276-305-4, pp. 354–361.
- [8] E. McConnell, D. McPolin, S. Taylor, Post-tensioning of glulam timber with steel tendons, *Constr. Build. Mater.* 73 (2014) 426–433. <https://doi.org/10.1016/j.conbuildmat.2014.09.079>
- [9] F. Wanninger, A. Frangi, Experimental and analytical analysis of a post-tensioned timber connection under gravity loads, *Eng. Struct.* 70 (2014) 117–129. <https://doi.org/10.1016/j.engstruct.2014.03.042>

- [10] T. Smith, F.C. Ponzo, A. Cesare, S. Pampanin, D. Carradine, A.H. Buchanan, D. Nigro, Post-tensioned glulam beam-column joints with advanced damping systems: testing and numerical analysis, *J. Earthquake Eng.* 18 (2014) 147–167. <https://doi.org/10.1080/13632469.2013.835291>
- [11] European Committee for Standardization (CEN), Timber structures – glued laminated timber and glued solid timber – requirements, EN 14080, 2013.
- [12] European Technical Assessment ETA-14/0349, 2014.
- [13] Eurocode: basis of structural design, EN 1990:2002/A1:2005/AC:2010.
- [14] Eurocode 5: design of timber structures. Part 1–1: general rules and rules for buildings, EN 1995-1-1:2004/AC:2006.
- [15] M. Saiidi, B. Douglas, S. Feng, Prestress force effect on vibration frequency of concrete bridges, *J. Struct. Eng. ASCE* 120 (1994) 2233–2241. [https://doi.org/10.1061/\(ASCE\)0733-9445\(1994\)120:7\(2233\)](https://doi.org/10.1061/(ASCE)0733-9445(1994)120:7(2233))
- [16] J. Kim, C. Yun, Y. Ryu, H. Cho, Identification of prestress-loss in PSC beams using modal information, *Struct. Eng. Mech.* 17 (2004) 467–482. [https://doi.org/10.12989/sem.2004.17.3\\_4.467](https://doi.org/10.12989/sem.2004.17.3_4.467)
- [17] Y. Zhang, R. Li, Natural frequency of full-prestressed concrete beam, *Trans. Tianjin Univ.* 13 (2007) 354–359. ISSN 1006-4982.